

Microwave Spectrum and Intramolecular Hydrogen Bonding of Propargyl Selenol ($\text{HC}\equiv\text{CCH}_2\text{SeH}$)

Harald Møllendal,^{*,†} Alexey Konovalov,[†] and Jean-Claude Guillemin^{‡,§}

Centre for Theoretical and Computational Chemistry (CTCC), Department of Chemistry, University of Oslo, P.O. Box 1033 Blindern, NO-0315 Oslo, Norway, École Nationale Supérieure de Chimie de Rennes, CNRS, UMR 6226, Avenue du Général Leclerc, CS 50837, 35708 Rennes Cedex 7, France, and Université européenne de Bretagne, 5 Boulevard Laënnec, 35000 Rennes, France

Received: February 9, 2010; Revised Manuscript Received: March 16, 2010

The microwave spectrum of propargyl selenol, $\text{HC}\equiv\text{CCH}_2\text{SeH}$, has been investigated in the 19–80 GHz spectral range at $-30\text{ }^\circ\text{C}$. The spectra of five isotopologues of one conformer, which has a synclinal conformation for the C–C–Se–H link of atoms, were assigned. This conformational preference allows for the formation of a weak intramolecular hydrogen bond between the hydrogen atom of the selenol group and the π electrons of the triple bond. This hydrogen-bonded conformer is at least 5 kJ/mol more stable than the rotamer having an antiperiplanar conformation for the C–C–Se–H chain. The microwave spectrum clearly shows that the hydrogen atom tunnels between the two mirror-image synclinal forms, but it was not possible to determine the tunneling frequency. The microwave study has been augmented by quantum chemical calculations at the MP2/aug-cc-pVTZ and B3LYP/aug-cc-pVTZ levels of theory. These calculations predict rotational and centrifugal distortion constants that are in good agreement with the experimental counterparts but predict a far too small energy difference of ≈ 1.5 kJ/mol for the energy difference between the antiperiplanar and synclinal forms. The conformational properties and internal hydrogen bonding of $\text{HC}\equiv\text{CCH}_2\text{SeH}$ are compared with similar properties of other selenols, which are stabilized by intramolecular hydrogen bonds.

Introduction

The ability of selenols to form intramolecular hydrogen (H) bonds in the gas phase was first demonstrated in the case of 3-buteneselenol ($\text{HSeCH}_2\text{CH}_2\text{C}=\text{CH}_2$),¹ where the H atom of the selenol group forms an internal H bond with the π electrons of the double bond. The next example was cyclopropylmethylselenol ($\text{C}_3\text{H}_5\text{CH}_2\text{SeH}$),² where the preferred form was found to be stabilized by a weak H bond between the selenol group and the pseudo- π electrons³ along the edge of the cyclopropyl ring. π electrons of the triple bond and the selenol group may also form a weak H-bonded system, as shown in the case of 3-butyne-1-selenol ($\text{HSeCH}_2\text{CH}_2\text{C}\equiv\text{CH}$).⁴ A fourth example is the recent study of 2-propene-1-selenol (allylselenol, $\text{HSeCH}_2\text{CH}=\text{CH}_2$), where the H atom of the selenol group interacts with the π electrons of the double bond in its preferred conformer.⁵

The present study of 2-propyne-1-selenol (propargyl selenol; $\text{HC}\equiv\text{CCH}_2\text{SeH}$) is an extension of our studies of the weak internal H bonding in selenols. The internal H bond in this compound is different from the previous four examples and involves the interaction between the selenol group with a triple bond in the β,γ -position. Propargyl selenol has also been chosen in order to allow a direct comparison of the H bonding abilities in the analogous alcohol (propargyl alcohol; $\text{HC}\equiv\text{CCH}_2\text{OH}$)⁶ and thiol (propargyl mercaptan; $\text{HC}\equiv\text{CCH}_2\text{SH}$),^{7–9} both of which are stabilized by intramolecular hydrogen bonding involving the π electrons of the triple bond in their lowest-energy conformers.

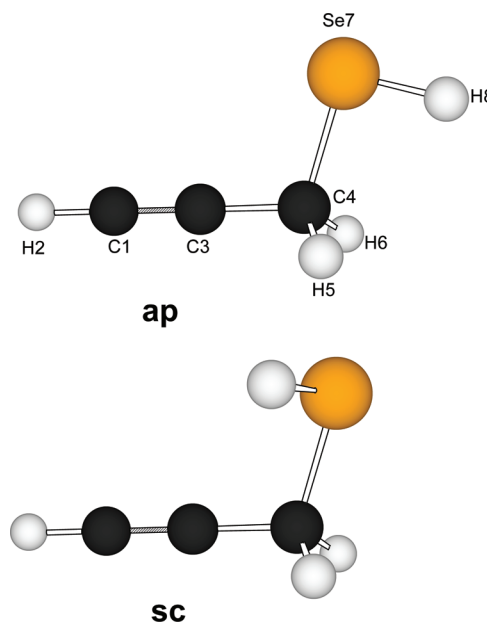


Figure 1. The antiperiplanar (**ap**) and synclinal (**sc**) conformers of $\text{HC}\equiv\text{CCH}_2\text{SeH}$. Atom numbering is indicated on **ap**.

A model of propargyl selenol with atom numbering is shown in Figure 1. Rotation about the C4–Se7 bond may produce rotational isomers. Two conformers, denoted **ap** and **sc**, with all-staggered atomic arrangements can be envisaged for this compound. In **ap**, the C3–C4–Se7–H8 link of atoms is antiperiplanar, whereas this chain is synclinal in **sc**. Interaction between the selenol group and the triple bond between C1 and C3 is possible in **sc**, whereas no such interaction can occur in **ap**. Mirror-image forms, which would have identical microwave

* To whom correspondence should be addressed: tel, +47 2285 5674; fax, +47 2285 5441; e-mail, harald.mollendal@kjemi.uio.no.

[†] University of Oslo.

[‡] École Nationale Supérieure de Chimie de Rennes.

[§] Université européenne de Bretagne.

(MW) spectra, exist for **sc**. The existence of such forms should lead to tunneling of the H atom of the selenol group between them. Interestingly, tunneling of the H atom of the hydroxyl and mercapto groups is a prominent feature of the MW spectra of the related compounds propargyl alcohol⁶ and propargyl mercaptan,^{7–10} where tunneling frequencies of 644319.69 and 6891.76(2) MHz have been reported for the *synclinal* forms of $\text{HC}\equiv\text{CCH}_2\text{OH}$ ⁶ and $\text{HC}\equiv\text{CCH}_2\text{SH}$,⁸ respectively.

This is the first MW study of propargyl selenol. The synthesis,¹¹ the photoelectron spectra,¹² and quantum chemical calculations¹² of the title compound have recently been reported, but no detailed conformational study was undertaken.

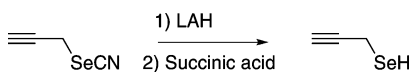
A successful investigation of a delicate conformational equilibrium such as the one presented by gaseous propargyl selenol requires experimental methods possessing high resolution. MW spectroscopy meets this requirement because of its superior accuracy and resolution, making this method especially well suited for conformational studies of gaseous species. The spectroscopic work has been augmented by high-level quantum chemical calculations, which were conducted with the purpose of obtaining information for use in assigning the MW spectrum and investigating properties of the potential-energy hypersurface.

This work also represents a continuation of our studies of intramolecular hydrogen bonding, of which 2-propene-1-selenol ($\text{HSeCH}_2\text{CH}=\text{CH}_2$),⁵ 3-butyne-1-selenol ($\text{HSeCH}_2\text{CH}_2\text{C}\equiv\text{CH}$),⁴ 4-pentyn-1-ol ($\text{HO}(\text{CH}_2)_3\text{C}\equiv\text{CH}$),¹³ trifluorothioacetic acid (CF_3COSH),¹⁴ (Z)-3-mercapto-2-propenenitrile ($\text{HSCH}=\text{CHC}\equiv\text{N}$),¹⁵ (Z)-3-amino-2-propenenitrile ($\text{H}_2\text{NCH}=\text{CHC}\equiv\text{N}$),¹⁶ 3-butyne-thiol ($\text{HSCH}_2\text{CH}_2\text{C}\equiv\text{CH}$),¹⁷ (methylenecyclopropyl)methanol ($\text{H}_2\text{C}=\text{C}_3\text{H}_3\text{CH}_2\text{OH}$),¹⁸ cyclopropylmethylselenol ($\text{C}_3\text{H}_5\text{CH}_2\text{SeH}$),² 2-chloroacetamide ($\text{CH}_2\text{ClCONH}_2$),¹⁹ 1,1,1-trifluoro-2-propanol ($\text{CF}_3\text{CH}(\text{OH})\text{CH}_3$),²⁰ cyclopropylmethylphosphine ($\text{C}_3\text{H}_5\text{CH}_2\text{PH}_2$),²¹ and 1-fluorocyclopropanecarboxylic acid ($\text{C}_3\text{H}_4\text{FCOOH}$),²² are recent examples. Less recent work on gas-phase studies of intramolecular H bonding is reviewed elsewhere.^{23,24}

Experimental Section

Preparation. *Caution: Propargyl selenol is potentially a highly toxic compound. All reactions and handling should be carried out in a well-ventilated hood.*

The synthesis of propargyl selenol has already been reported.¹¹ The compound was prepared by a chemoselective reduction of propargyl selenocyanate with LAH in tetraglyme, followed by the reaction of the crude mixture with succinic acid.



Microwave Experiment. The spectrum of propargyl selenol was studied in the 19–80 GHz frequency interval by Stark-modulation spectroscopy, using the microwave spectrometer of the University of Oslo, which measures the frequency of isolated transitions with an estimated accuracy of ≈ 0.10 MHz. Details of the construction and operation of this spectrometer have been given elsewhere.^{22,25} While the spectrum was recorded, the Stark cell was cooled to approximately -30°C with solid CO_2 , in an attempt to increase the intensity of the spectrum. Radio frequency microwave double-resonance (RFMWDR) experiments, similar to those performed by Wodarczyk and Wilson,²⁶ were also conducted to assign unambiguously particular transitions. Propargyl selenol is kinetically unstable and was therefore stored at liquid-nitrogen (-196°C) or dry ice (-78°C) temperature. The sample had to be heated to roughly 0°C in

order to fill the cell with fresh sample. The compound polymerizes readily, and this was observed during one of these heating processes. The spectra were taken at a vapor pressure of approximately 10 Pa. No decomposition was observed for the gaseous species at about -30°C .

Quantum Chemical Methods. A series of quantum-chemical calculations were conducted on propargyl selenol using the Gaussian03 suite of programs,²⁷ running on the Titan cluster at the University of Oslo. The effects of electron correlation were included by the use of density functional theory (DFT), as well as second-order Møller–Plesset perturbation theory (MP2).²⁸ The calculations were performed using the aug-cc-pVTZ basis set,^{29,30} which is of triple- ζ quality and includes polarized functions for valence electrons and is augmented by diffuse functions. DFT optimizations were undertaken employing the B3LYP hybrid functional.^{31,32} The default convergence criteria of Gaussian03 were observed. The results of the B3LYP and MP2 calculations will be compared with one another and with the experimental findings.

Results

Quantum Chemical Calculations. A B3LYP potential function for rotation about the C4–Se7 bond was first calculated by varying the C3–C4–Se7–H8 dihedral angle in steps of 10° , allowing all other structural parameters to vary freely. These calculations indicated that there are two minima corresponding to the **ap** and **sc** conformers, as well as two maxima (transition states) at 0 and approximately 120° of said dihedral angle. The B3LYP structures, energies, dipole moments, harmonic and anharmonic vibrational frequencies, and centrifugal distortion constants were then calculated for **ap** and **sc**, whereas the structures, energies, and harmonic vibrational frequencies were computed for the two transition states. No imaginary vibrational frequencies were calculated for both **ap** and **sc**, which indicate that they are minima (“stable conformers”) on the potential energy hypersurface. However, one imaginary vibrational frequency, associated with the torsion about the C4–Se7 bond, was found for each of the two transition states, characterized by the dihedral C3–C4–Se7–H8 being 0 or 123.5° .

The *synclinal* rotamer, **sc**, which was calculated to have a dihedral C3–C4–Se7–H8 angle of 59.9° , is predicted to be the global minimum and to have an electronic B3LYP energy that is 1.42 kJ/mol lower than that of **ap**, characterized with the C3–C4–Se7–H8 dihedral angle being exactly 180° . Inclusion of zero-point vibrational energies changes this energy difference slightly to 1.21 kJ/mol. The maxima were calculated to have 4.36 (0°) and 4.73 kJ/mol (123.5°) higher electronic energies than **sc**. The full potential function could now be drawn, as shown in Figure 2. This function is a typical double-minimum function, which implies that tunneling between the two mirror images of **sc** at 59.9 and 300.1° should manifest itself in the MW spectrum in a similar manner as observed for the *synclinal* forms of $\text{HC}\equiv\text{CCH}_2\text{OH}$ ⁶ and $\text{HC}\equiv\text{CCH}_2\text{SH}$.^{7–9}

MP2 calculations are much more costly than the B3LYP calculations and only the energies, structures, dipole moments, vibrational frequencies, and centrifugal distortion constants were therefore calculated for **ap** and **sc**. The latter conformer was calculated to be the more stable by 1.76 kJ/mol after corrections for zero-point energies.

The MP2 and B3LYP structures of **ap** and **sc** are listed in Table 1. The rotational constants calculated from these structures are shown in Table 2, together with Watson’s *S*-reduction quartic centrifugal distortion constants,³³ the components of the dipole moment along the principal inertial axes, and the energy

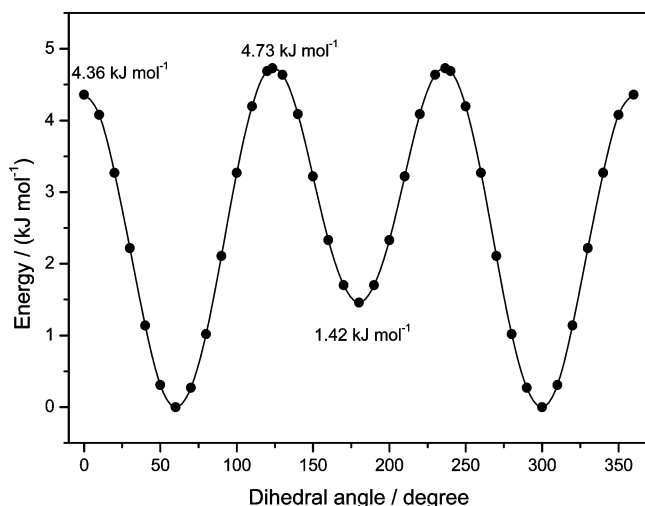


Figure 2. The B3LYP/aug-cc-pVTZ potential function for rotation about the C4–Se7 bond. Relative energies are indicated on the ordinate and values of the C3–C4–Se7–H8 dihedral angle are indicated on the abscissa. A dihedral angle of 0° corresponds to a synperiplanar conformation for the C3–C4–Se7–H8 link of atoms.

TABLE 1: MP2 and B3LYP Geometries^a of the **ap and **sc** Conformers of HC≡CCH₂SeH**

	MP2		B3LYP	
	ap	sc^b	ap	sc^b
Bond Length (pm)				
C1–H2	106.2	106.2	106.1	106.1
C1–C3	121.5	121.6	119.9	120.0
C3–C4	144.9	144.8	144.4	144.3
C4–H5	108.7	108.7	108.7	108.7
C4–H6	108.7	108.9	108.7	108.9
C4–Se7	196.0	195.7	200.4	199.9
Se7–H8	145.5	145.3	147.4	147.1
Angle (deg)				
C3–C4–H5	110.8	111.4	111.2	111.6
C3–C4–H6	110.8	111.0	111.2	111.4
C3–C4–Se7	108.1	112.6	109.5	113.9
H5–C4–H6	109.8	108.4	109.5	108.2
H5–C4–Se7	108.6	108.6	107.7	107.6
H6–C4–S7	108.6	104.5	107.7	103.7
C4–Se7–C8	94.1	93.6	94.1	94.4
H2–C1–C3	179.8	179.6	179.8	179.8
C1–C3–C4	178.9	179.0	179.5	179.3
H2–C4–Se7	107.6	112.4	109.3	113.9
C1–C4–Se7	107.7	112.5	109.3	113.9
Dihedral Angle (deg)				
C3–C4–Se7–H8	180.0	57.2	180.0	59.9
H5–C4–Se7–H8	59.7	−66.6	59.0	−64.4
H6–C4–Se7–H8	−59.7	177.8	−59.0	−178.9

^a Basis set: aug-cc-pVTZ.^{29,30} ^b The MW spectrum of **ac** (in boldface) was assigned.

differences relative to the energy of the global minimum conformer **sc**. The B3LYP calculations yielded the vibration–rotation constants (the α values).³⁴ The B3LYP harmonic frequencies and the α values are shown in Tables 1S in the Supporting Information.

The MP2 and B3LYP results warrant comments. There are some noteworthy differences in the structures calculated by these two methods, particularly associated with the selenol group. The B3LYP C4–Se7 bond length (Table 1) is about 4 pm longer than the MP2 bond length (Table 1) and the B3LYP Se7–H8 bond length is approximately 2 pm longer than its MP2 counterpart. Experimental C–Se and Se–H bond lengths of

TABLE 2: Theoretical^a Spectroscopic Parameters of HC≡CCH₂⁸⁰SeH

	MP2		B3LYP	
	ap	sc^b	ap	sc^b
Rotational Constants (MHz)				
<i>A</i>	18427.5	19430.6	18792.8	19776.2
<i>B</i>	2220.7	2117.8	2145.6	2052.6
<i>C</i>	2006.9	1953.7	1949.4	1903.1
Quartic Centrifugal Distortion Constants ^c (kHz)				
<i>D_J</i>	1.12	0.888	1.01	0.797
<i>D_{JK}</i>	−17.1	−30.0	−16.3	−27.1
<i>D_K</i>	253	429	260	429
<i>d₁</i>	−0.196	−0.157	−0.167	−0.130
<i>d₂</i>	−0.0136	−0.00435	−0.0109	−0.00339
Principal Inertial Axes Dipole Moment Components ^d (10 ^{−30} C m)				
μ_a	4.3	2.4	3.8	2.1
μ_b	1.7	1.7	1.7	1.7
μ_c	0.0	1.7	0	1.4
Energy Difference ^e (kJ/mol)				
ΔE	1.76	0.0	1.20	0.0

^a Basis set: aug-cc-pVTZ.^{29,30} ^b The microwave spectrum of this conformer was assigned. ^c *S*, reduction; *I*⁺, representation.³³ ^d 1 D = 3.33564 × 10^{−30} C m. ^e Relative to **sc** and corrected for zero-point vibrations. MP2 electronic energy of **sc**: −6607 079.47 kJ/mol. B3LYP electronic energy of **sc**: 6611 8706.62 kJ/mol.

related compounds have been reported. The *r*₀ C–Se bond length in CH₃SeH is 195.9 pm.³⁵ The *r*_s C–Se bond length is 195.7(4) pm in the C–C–Se–H synclinal conformer of CH₃CH₂SeH and 196.2(2) pm in the antiperiplanar form.³⁶ It is seen from Table 1 that these experimental C–Se bond lengths are much closer to the MP2 predictions than to the B3LYP results. The Se–H bond length is 147.3 pm in CH₃SeH,³⁵ 146.7(4) pm in the C–C–Se–H synclinal form of CH₃CH₂SeH,³⁶ and 144.0(10) pm in the antiperiplanar conformation of the latter compound.³⁶ These experimental results are not far from both the MP2 and B3LYP predictions appearing in Table 1.

The two methods predict the bond angles to be rather similar. The largest discrepancies are found for the bond angles associated with the selenol group, where deviations of ≈1.5° are seen (Table 1). Larger differences are seen for the dihedral angles. The C3–C4–Se7–H8 dihedral angle of **sc** is 2.7° smaller in the MP2 than in the B3LYP calculations. This brings the H atom of the selenol group into closer proximity with the π electrons of the C1≡C2 triple bond in the MP2 than in the B3LYP structure, as can be seen from the nonbonded H8⋯C1 and H8⋯C2 distances, whose MP2 values are 293.0 and 369.6 pm, respectively, compared to 303.7 and 381.1 pm (B3LYP). The MP2 method therefore seems to indicate a stronger H-bond interaction than the B3LYP method does.

The quartic centrifugal distortion constants predicted by the two methods (Table 2) are in fairly good agreement in the cases of *D_J*, *D_{JK}*, and *D_K*, whereas relatively larger differences are seen for *d₁* and *d₂*. This is not surprising since they depend on the second derivative at the minima of the potential energy hypersurface. The B3LYP dipole moments (same table) are generally somewhat smaller than their MP2 counterparts, which is typical, whereas the two theoretical methods predict similar and small energy differences ≈1.5 kJ/mol between **ap** and **sc**.

Microwave Spectrum and Assignment of **sc.** The relatively small energy difference predicted for the two forms would imply that both rotamers should be present in significant concentrations at −30 °C. **sc** has a statistical weight of 2 relative to **ap**, whose

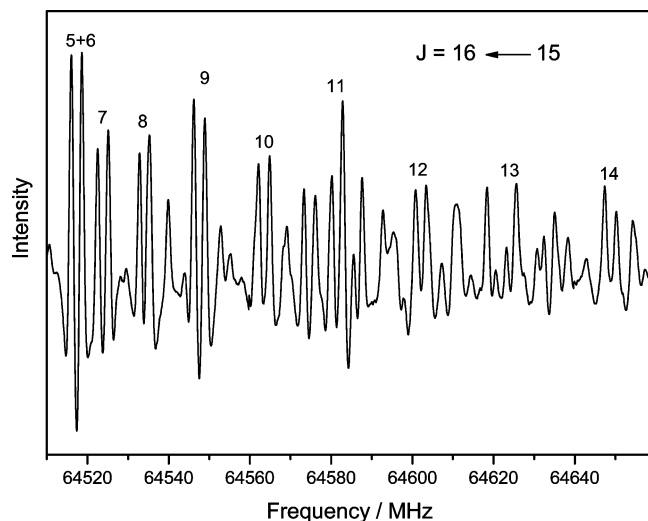


Figure 3. MW spectrum of the $J = 16 \leftarrow 15$ pile-up region taken at a Stark field strength of approximately 110 V/cm. The K_{-1} pseudo quantum number is indicated above each pair of lines of approximately equal intensity, which are assumed to belong to the 0^+ and 0^- states. The $K_{-1} = 5$ and $K_{-1} = 6$ of the two states coalesce in this particular case into the two strongest lines shown to the far left in this figure.

statistical weight is 1. μ_a is the largest dipole moment component of each conformer, and this component is calculated to be about twice as large in **ap** as compared to **sc** (Table 2). This favors the intensity of the spectrum of **ap** by a factor of 4 compared to **sc**, because intensities depend on the square of the dipole moment component. The a -type spectra of **ap** would therefore be roughly as intense as the spectrum of **sc**, provided the theoretical calculations of the energy difference (≈ 1.5 kJ/mol; Table 2) were correct.

The values of the *largest* dipole moment component, μ_a , of each rotamer are only roughly 4×10^{-30} C m for **ap**, and 2×10^{-30} C m for **sc** (Table 2), which means that the absolute intensity of the spectrum would not be high for either rotamer. Another factor that affects to the intensity negatively is the fact that selenium has six naturally occurring isotopes, of which five are relatively abundant (^{76}Se (9.0%), ^{77}Se (7.6%), ^{78}Se (23.5%), ^{80}Se (49.8%), and ^{82}Se (9.2%)), which means that the intensity is reduced accordingly because the intensity of the spectrum of each isotopologue is proportional to its concentration.

Survey spectra demonstrated that propargyl selenol indeed has a relatively weak, but rich, spectrum, as expected. The fact that μ_a is the major dipole moment component of each rotamer implies that the spectrum of each of them should be dominated by strong aR transitions. Both **ap** and **sc** are nearly prolate rotors with Ray's asymmetry parameter³⁷ $\kappa \approx -0.98$, and this should lead to series of pile-ups of aR -branch transitions in the 40–80 GHz interval separated by approximately $B + C$. Most of the transitions found in the pile-up regions would be modulated at comparatively low Stark voltages because the corresponding K_{-1} pairs of the aR transitions are practically degenerate. Several pile-up series were readily observed in the low-voltage survey spectra in accord with these predictions. The strongest of these pile-ups, with $B + C \approx 4.04$ GHz, was assumed to belong to the spectrum of the ^{80}Se isotopologue of either **ap** or **sc**. A typical example of one such pile-up is shown in Figure 3. Similar, but weaker, pile-ups were also observed for the ^{76}Se , ^{77}Se , ^{78}Se , and ^{82}Se isotopologues of one of the rotamers.

Closer inspection revealed that these pile-ups all have a complicated and characteristic fine structure. One striking feature is pairs of lines of roughly equal intensities seen for each K_{-1}

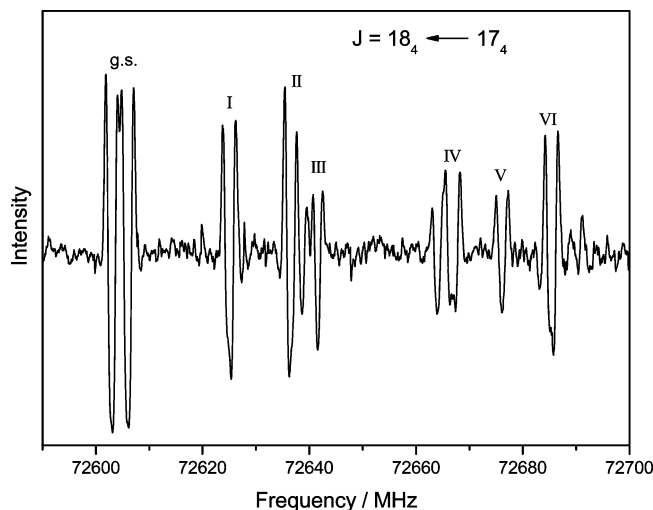


Figure 4. The RFMWDR spectrum of the $J = 18 \leftarrow 17$ $K_{-1} = 4$ pairs, which are separated by approximately 2.2 MHz. The rf employed in this case was 3.31 MHz. The pairs denoted g.s. belong to the 0^+ and 0^- states, whereas the remaining pairs designated by Roman numerals belong to vibrationally excited states.

transition. This fine-structure is evident in Figure 3, where the values of the K_{-1} pseudo quantum number are indicated above each such pair. Similar doublets have been observed for the aR spectra of the synclinal forms of $\text{HC}\equiv\text{CCH}_2\text{OH}$ ⁶ and $\text{HC}\equiv\text{CCH}_2\text{SH}$ ^{7–9} and assigned to the symmetrical (0^+) and antisymmetrical (0^-) species, respectively, of the ground vibrational state.^{6–10} These two symmetry species exist because both the alcohol⁶ and the thiol^{7–9} have a double-minimum potential associated with the rotation about the C–O or C–S bonds, respectively. The doublet structure of each aR -pair is one piece of evidence that the observed pile-ups indeed belong to **sc** and not to **ap**, which would not be expected to have this kind of fine structure.

The very specific RFMWDR technique was then employed in an attempt to obtain an unambiguous assignment of the spectrum. An example of a RFMWDR spectrum of the $J = 18 \leftarrow 17$ pile-up is shown in Figure 4. In this case, the two $J = 18_4 \leftarrow 17_4$ transitions, which are slightly split by asymmetry, have been modulated. The quartet of lines to the far left in this figure belongs to the 0^+ and 0^- states of these two $K_{-1} = 4$ transitions. Several vibrationally excited state spectra of the $J = 18_4 \leftarrow 17_4$ transitions also appear as shown in Figure 4, where they have been denoted by Roman numerals. These excited states are discussed below.

Similar RFMWDR spectra to that shown in Figure 4 were obtained for several other $K_{-1} = 3$ and $K_{-1} = 4$ aR transitions, which were assigned in this manner. The assignments were gradually extended to additional aR transitions and fitted to the Watson S reduction Hamiltonian³³ using Sørensen's program Rotfit.³⁸ Overlapping lines were frequently encountered especially in the pile-up regions, because several vibrationally excited states occur, as Figure 4 clearly shows, and because lines with different K_{-1} of both the 0^+ and the 0^- species occasionally overlap. The overlapping lines were given lower weights than isolated transitions in the weighted least-squares fits.

The μ_b dipole moment component of **sc** is computed to have roughly 70% of the value of μ_a (Table 2). The transitions of the $K_{-1} = 1 \leftarrow 0$, $2 \leftarrow 1$, and $3 \leftarrow 2$ bQ -branch series should be among the strongest b -type lines occurring in the investigated spectral range. The spectroscopic constants obtained from the aR lines were used to predict the frequencies of these transitions,

TABLE 3: Spectroscopic Constants^a of HC≡CCH₂⁷⁸SeH and HC≡CCH₂⁸⁰SeH^b

	HC≡CCH ₂ ⁷⁸ SeH		HC≡CCH ₂ ⁸⁰ SeH	
	0 ⁺	0 ⁻	0 ⁺	0 ⁻
<i>A</i> (MHz)	19488.166(61)	19498.57(11)	19470.648(39)	19480.899(94)
<i>B</i> (MHz)	2109.9575(17)	2110.1055(16)	2095.3599(16)	2095.5065(17)
<i>C</i> (MHz)	1946.7611(17)	1946.7716(16)	1934.1653(16)	1934.1734(17)
<i>D_J</i> (kHz)	0.8909(31)	0.8909(28)	0.8789(31)	0.8755(30)
<i>D_{JK}</i> (kHz)	-29.423(12)	-29.453(11)	-29.156(9)	-29.182(9)
<i>D_K</i> (kHz)	455.2(79)	489.2(80)	466.0(45)	502.4(67)
<i>d₁</i> (kHz)	-0.15412(34)	-0.15273(38)	-0.15069(12)	-0.15022(23)
<i>d₂</i> (kHz)	-0.00377(17)	-0.00473(16)	-0.003711(51)	-0.004308(96)
Δ ^c (10 ⁻²⁰ u m ²)	-5.85363(11)	-5.824403(95)	-5.855049(65)	-5.825602(75)
no. of transitions ^d	154	153	215	211
rms ^e	1.300	1.176	1.411	1.524

^a *S*, reduction; *I*, representation.³³ Uncertainties represent 1 standard deviation. ^b Spectra of the ⁷⁸Se isotopologue are listed in Tables 6S and 7S. Spectra of the ⁸⁰Se isotopologue are listed in Tables 8S and 9S in the Supporting Information. ^c Δ = *I_c* - *I_a* - *I_b*. Conversion factor 505379.05 MHz 10⁻²⁰ u m². ^d Number of transitions. ^e Root-mean-square of a weighted fit.

which were found to occur in pairs of lines of equal intensity that were split by several megahertz. The *b*-type spectrum was so weak that it was only possible to make unambiguous assignments for members of said *Q*-branch series.

The *c*-axis dipole moment component of **ac** is calculated to be roughly as large as μ_b (Table 2). The spectroscopic constants obtained from the *R*- and *Q*-branch transitions were employed to predict the frequencies of the strongest *c*-type transitions in the spectrum, which were not found at their predicted frequencies. The reason for this is a change of selection rules from normal behavior. The *c* dipole in these systems is a transition moment that leads to transitions between 0⁺ and 0⁻ states since the *c* dipole is an odd operator and the product of the levels it connects must therefore be odd. Thus the *c*-transition frequencies will be offset by ±Δ and this tunneling frequency has been observed as 644319.69 MHz in HC≡CCH₂OH⁶ and 6891.76(2) MHz in HC≡CCH₂SH.⁸ It is difficult to predict what Δ would be in the present case. Tunneling frequencies of selenols have only been determined in a few cases. It is 1083.33(4) MHz in the synclinal conformation of CH₃CH₂SeH³⁶ compared to 1753.84(29) MHz its thiol congener, CH₃CH₂SH.³⁹ A value of several gigahertz was therefore expected for Δ in the case of the title compound in analogy with the findings for ethaneselenol³⁶ and ethanethiol.³⁹ Many unsuccessful attempts were made to assign these weak *c*-type transitions in order to determine the tunneling frequency.

The spectra of 0⁺ and 0⁻ species of the ⁸⁰Se isotopologue are shown in Tables 8S and 9S, respectively, in the Supporting Information and the spectroscopic constants from the *a*- and *b*-type transitions are listed in Table 3. It is not obvious which spectrum belongs to each of the two symmetry species. Our main reason for making the present symmetry species assignments is that the pseudo inertial defect Δ (not to be confused with the tunneling frequency) is given by Δ = *I_c* - *I_a* - *I_b* = -5.855049(65) × 10⁻²⁰ u m² for the 0⁺-species is slightly larger in magnitude than Δ = -5.825602(75) × 10⁻²⁰ u m² for the 0⁻ species (Table 3), because it would be expected that Δ decreases toward -3.2 × 10⁻²⁰ u m² as the C3-C4-Se7-H8 dihedral angle approaches 180°. However, the reverse symmetry assignment cannot be excluded.

Comparison of the theoretical (Table 2) and experimental (Table 3) spectroscopic constants is in order. It is seen from these two tables that the experimental value of the MP2 *A* rotational constant of the 0⁺ species is 0.2% smaller and the *B* and *C* rotational constants are about 1% larger than the experimental rotational constants. The B3LYP *A* rotational

constant is 1.5% larger; the *B* and *C* constants are 2% and 1.6%, respectively, smaller than their experimental counterparts. Differences of this order of magnitude have to be expected because the experimental and theoretical rotational constants are defined differently. The experimental constants are *effective* parameters, which mean that they are averaged over the vibrational state, whereas the MP2 and B3LYP constants are calculated from an approximate equilibrium structure. It is difficult to say on the basis of the rotational constants which structure is better, but the agreement is best for the MP2 structure. Interestingly, it has been demonstrated that MP2 structures obtained using large basis sets are rather close to the equilibrium structures.⁴⁰

There is very good agreement between the experimental and MP2 centrifugal distortion constants. The agreement between the experimental and B3LYP centrifugal distortion constants is also satisfactory.

Assignment of Further Isotopologue of **sc.** The ground-state spectra of the 0⁺ and 0⁻ species of ⁷⁶Se (9.0%; Tables 2S and 3S in Supporting Information), ⁷⁷Se (7.6%; Tables 4S and 5S in Supporting Information), ⁷⁸Se (23.5%; Tables 6S and 7S in Supporting Information), and ⁸²Se (9.2%; Tables 10S and 11S in Supporting Information) isotopologues were predicted using the MP2 structure in Table 2 to obtain shifts in the rotational constants upon substitution of the parent ⁸⁰Se atom with the other alternatives. These shifts were added to the experimental rotational constants of Table 3 and used to predict the spectra of the isotopologues, which were readily assigned. It was possible to assign the *a*- and *b*-type spectra for the ⁷⁸Se isotopologue, whereas only the *a**R* spectra were assigned for the remaining less abundant isotopologues because the *b*-type lines are too weak. The spectroscopic constants are shown in Table 3 for the ⁷⁸Se species, while the spectroscopic constants of the less abundant species are listed in Table 4.

Kraitchman's coordinates⁴¹ of the selenium atom calculated from 0⁺ and 0⁻ species using the ⁷⁸Se and ⁸⁰Se isotopologues are in good agreement with coordinates calculated from the MP2 structure, which is additional evidence that the spectrum of **sc** has indeed been assigned.

Only a very inaccurate *A* rotational constant and no significant values for the *D_K*, *d₁*, and *d₂* centrifugal distortion constants could be obtained from the *a*-type lines of ⁷⁶Se, ⁷⁷Se, and ⁸²Se isotopologues. The *A* constants, which were estimated from the shifts of the rotational constants upon substitution as described above, were therefore held fixed in the least-squares fits. The *D_K*, *d₁*, and *d₂* constants were also fixed at the experimental

TABLE 4: Spectroscopic Constants^a of HC≡CCH₂⁷⁶SeH, HC≡CCH₂⁷⁷SeH, and HC≡CCH₂⁸²SeH^b

	HC≡CCH ₂ ⁷⁶ SeH		HC≡CCH ₂ ⁷⁷ SeH		HC≡CCH ₂ ⁸² SeH	
	0 ⁺	0 ⁻	0 ⁺	0 ⁻	0 ⁺	0 ⁻
<i>A</i> (MHz)	19507.5 ^c	19517.8 ^c	19497.9 ^c	19508.2 ^c	19453.4 ^c	19463.7 ^c
<i>B</i> (MHz)	2124.226(93)	2124.24(19)	2116.31(13)	2116.95(12)	2080.99(15)	2079.47(18)
<i>C</i> (MHz)	1961.036(95)	1961.17(20)	1954.50(13)	1954.02(12)	1922.56(16)	1924.30(19)
<i>D_J</i> (kHz)	0.8872(47)	0.8719(59)	0.8640(60)	0.8801(44)	0.8495(44)	0.8415(50)
<i>D_{JK}</i> (kHz)	-29.463(17)	-29.476(22)	-29.289(21)	-29.381(16)	-28.940(30)	-28.716(18)
Δ^d (10 ⁻²⁰ u m ²)	-6.109(23)	-6.111(48)	-6.149(31)	-6.000(29)	-5.966(39)	-6.368(47)
no. of transitions ^e	84	70	86	82	76	84
rms ^f	0.920	1.073	1.294	0.932	0.860	0.932

^a *S*, reduction; *I'*, representation.³³ Uncertainties represent 1 standard deviation. *D_K*, *d*₁, and *d*₂ centrifugal distortion constants have been fixed at the values obtained for the 0⁺ or 0⁻ species of the ⁸⁰Se isotopologue; see text. ^b Spectra of the ⁷⁶Se isotopologue are listed in Tables 2S and 3S. Spectra of the ⁷⁷Se isotopologue are listed in Tables 4S and 5S, and spectra of the ⁸²Se isotopologue are listed in Tables 10S and 11S in the Supporting Information. ^c Fixed; see text. ^d $\Delta = I_c - I_a - I_b$. Conversion factor 505379.05 MHz 10⁻²⁰ u m². ^e Number of transitions. ^f Root-mean-square of a weighted fit.

TABLE 5: Spectroscopic Constants^a of Vibrationally Excited States of HC≡CCH₂⁸⁰SeH

	I	II	III	IV	V	VI
<i>B</i> (MHz)	2097.49(18)	2097.60(20)	2095.58(22)	2099.27(47)	2098.10(38)	2097.66(37)
<i>C</i> (MHz)	1933.08(20)	1933.64(22)	1936.17(24)	1933.55(52)	1935.40(42)	1936.44(41)
Δ^b (10 ⁻²⁰ u m ²)	-5.464(49)	-5.527(53)	-6.101(58)	-5.32(12)	-5.71(10)	-5.897(47)
no. of transitions ^c	14	14	7	8	6	11
rms ^d	1.977	2.281	1.1792	2.677	1.392	3.385

^a *S*, reduction; *I'*, representation.³³ Uncertainties represent 1 standard deviation. The *A* rotational constant and the centrifugal distortion constants have been kept constant in the least-squares fit at the value shown for the 0⁺ species of the ⁸⁰Se isotopologue (Table 3). The spectra are listed in Tables 12S–17S in the Supporting Information. ^b $\Delta = I_c - I_a - I_b$. Conversion factor 505379.05 MHz 10⁻²⁰ u m². ^c Number of transitions. ^d Root-mean-square of a weighted fit.

values found for 0⁺ or 0⁻ species of the ⁸⁰Se isotopologue because they cannot be determined accurately from the ^a*R* spectra. The spectroscopic constants obtained in this manner are collected in Table 4.

Vibrationally Excited States of *sc*. At least six vibrationally excited states could be seen in the RFMWDR spectra (see Figure 4). Unambiguous assignments could only be made for the ^a*R* lines of six excited states that were modulated using this technique, because of the complicated nature of the pile-ups. Determination of their frequencies by relative intensity measurements was not possible for the same reasons. The spectra are listed in Tables 12S–17S in the Supporting Information. The spectroscopic constants appearing in Table 5 have been obtained by fixing the *A* rotational constants and the centrifugal distortion constants to the experimental values of the 0⁺ state (Table 3) in the least-squares fits.

Assignments of these excited states to vibrational modes are not straightforward. The lowest fundamental is a bending vibration with a harmonic frequency of 152 cm⁻¹ according to the B3LYP calculations (Table 1S), whereas the second lowest fundamental is the torsion about the C4–Se7 bond at 183 cm⁻¹ (Table 1S). The next mode, which is a bending vibration, is calculated to have a frequency of 339 cm⁻¹ (same table). The experimental vibration–rotation constants calculated for the vibrational modes (not given herein) are not in good agreement with the B3LYP counterparts shown in Table 1S, so there is not much help to gain from them. However, torsion about the C4–Se7 bond is not expected to change the rotational constants very much because little reduced mass is involved in this motion. It is therefore very tentatively assumed that strongest excited states, namely, I and II, might be 1⁺ and 1⁻ states, whereas III, IV, V, and VI could belong to excited states of low-frequency bending vibrations.

Searches for *ap*. The best way to assign the spectrum of this hypothetical rotamer would presumably have been from a spectrum taken at low Stark voltages, since ^a*R* pile-ups would

be expected for this form, as mentioned above. It is also expected that the MP2 rotational constants calculated for **ap** would be quite accurate, just as in the case of **sc**. However, there is no indication in the spectrum of the presence of this rotamer. It is assumed that it would have been assigned had its spectrum had an intensity similar to that of the spectrum of the ⁷⁶Se or ⁸²Se isotopologues of **sc** (9%). Because μ_a of **ap** would be twice as large as μ_a of **sc**, it is concluded that 4% of **ap** is definitely a maximum concentration of this species at -30 °C. The energy difference between **ap** and **sc** must therefore be at least 5 kJ/mol. This value has been obtained assuming a Boltzmann distribution for the energy and statistical weight of 1 for **ap** relative to 2 for **sc**. This energy difference is at variance with the MP2 value (1.76 kJ/mol; Table 2) and the B3LYP result (1.20 kJ/mol). It therefore appears that the two theoretical methods underestimate the stabilization of **sc** by several kJ/mol. This is not surprising given the relatively large number (34) of electrons of the selenium atom.

Discussion

The microwave spectrum of HC≡CCH₂SeH demonstrates that **sc** is at least 5 kJ/mol more stable than **ap**. The H atom of the selenol group is brought into close proximity with the π electrons in **sc**, which may be therefore be stabilized by a weak intramolecular H bond. This situation parallels the findings made for HSeCH₂CH₂C≡CH,¹ cyclopropylmethylselenol (C₃H₅CH₂SeH),² HSeCH₂CH₂C≡CH,⁴ and HSeCH₂CH=CH₂,⁵ where the H atom interacts with the π electrons^{1,4,5} or the pseudo π electrons² in each case, with the result that the H-bonded form is also the most stable conformer of each of these compounds.

The distances between the H atom of the selenol group and the nearest carbon atom having a double or triple bond is 292 pm in HSeCH₂CH₂CH=CH₂,¹ 273 pm in HSeCH₂CH₂C≡CH,⁴ and 292 pm in HSeCH₂CH=CH₂.⁵ The distance between the corresponding H atom in cyclopropylmethylselenol and the

midpoint of the nearest C–C bond of the cyclopropyl ring is 291 pm.² These distances are very similar to the MP2 distance of 293 pm in the title compound between the H atom in question and the nearest carbon atom having a triple bond.

Interestingly, the sum, 290 pm, of the van der Waals radii of the half-thickness of aromatic carbon (170 pm) and H (120 pm)⁴² is close to the nonbonded distances of the internal H-bonded examples above, which is an indication that these H bonds are indeed weak. It is therefore assumed that the remarkable stability of **sc** over **ap** by at least 5 kJ/mol cannot be explained by considering only the internal H bond. Additional effects must be partly responsible for this conformational preference. One possibility is the interaction between electrons of the selenol atom and the electrons of the triple bond. Repulsion between these electron clouds appears to be more prominent in **ap** compared to **sc** because the maximum electron density on the selenium atom is oriented more directly toward the triple bond in **ap**. It is therefore suggested that this repulsion in combination with the internal H bond makes **sc** at least 5 kJ/mol more stable than **ap**.

Acknowledgment. We thank Anne Horn for her skillful assistance. The Research Council of Norway (Program for Supercomputing) is thanked for a grant of computer time. A.K. thanks The Research Council of Norway for financial assistance through Contract 177540/V30. J.-C.G. thanks the Centre National d'Etudes Spatiales (CNES) for financial support.

Supporting Information Available: Results of the theoretical calculations and the microwave spectra. This material is available free of charge via the Internet at <http://pubs.acs.org>.

References and Notes

- (1) Petitprez, D.; Demaison, J.; Włodarczyk, G.; Guillemin, J.-C.; Møllendal, H. *J. Phys. Chem. A* **2004**, *108*, 1403.
- (2) Cole, G. C.; Møllendal, H.; Guillemin, J.-C. *J. Phys. Chem. A* **2006**, *110*, 2134.
- (3) Walsh, A. D. *Trans. Faraday Soc.* **1949**, *45*, 179.
- (4) Møllendal, H.; Mokso, R.; Guillemin, J.-C. *J. Phys. Chem. A* **2008**, *112*, 3053.
- (5) Møllendal, H.; Kononov, A.; Guillemin, J.-C. *J. Phys. Chem. A* **2009**, *113*, 6342.
- (6) Hirota, E. *J. Mol. Spectrosc.* **1968**, *26*, 335.
- (7) Bolton, K.; Sheridan, J. *Spectrochim. Acta, Part A* **1970**, *26*, 1001.
- (8) Scappini, F.; Mäder, H.; Sheridan, J. *Z. Naturforsch., A* **1973**, *28*, 77.
- (9) Scappini, F.; Favero, P. G.; Cervellati, R. *Chem. Phys. Lett.* **1975**, *33*, 499.
- (10) Mirri, A. M.; Scappini, F.; Cervellati, R.; Favero, P. G. *J. Mol. Spectrosc.* **1976**, *63*, 509.
- (11) Riague, E. H.; Guillemin, J.-C. *Organometallics* **2002**, *21*, 68.
- (12) Guillemin, J.-C.; Bajor, G.; Riague, E. H.; Khater, B.; Veszprémi, T. *Organometallics* **2007**, *26*, 2507.

- (13) Møllendal, H.; Dreizler, H.; Sutter, D. H. *J. Phys. Chem. A* **2007**, *111*, 11801.
- (14) Møllendal, H. *J. Phys. Chem. A* **2007**, *111*, 1891.
- (15) Cole, G. C.; Møllendal, H.; Khater, B.; Guillemin, J.-C. *J. Phys. Chem. A* **2007**, *111*, 1259.
- (16) Askeland, E.; Møllendal, H.; Uggerud, E.; Guillemin, J.-C.; Aviles Moreno, J.-R.; Demaison, J.; Huet, T. R. *J. Phys. Chem. A* **2006**, *110*, 12572.
- (17) Cole, G. C.; Møllendal, H.; Guillemin, J.-C. *J. Phys. Chem. A* **2006**, *110*, 9370.
- (18) Møllendal, H.; Frank, D.; De Meijere, A. *J. Phys. Chem. A* **2006**, *110*, 6054.
- (19) Møllendal, H.; Samdal, S. *J. Phys. Chem. A* **2006**, *110*, 2139.
- (20) Møllendal, H. *J. Phys. Chem. A* **2005**, *109*, 9488.
- (21) Cole, G. C.; Møllendal, H.; Guillemin, J.-C. *J. Phys. Chem. A* **2005**, *109*, 7134.
- (22) Møllendal, H.; Leonov, A.; de Meijere, A. *J. Phys. Chem. A* **2005**, *109*, 6344.
- (23) Wilson, E. B.; Smith, Z. *Acc. Chem. Res.* **1987**, *20*, 257.
- (24) Møllendal, H. *NATO ASI Ser., Ser. C* **1993**, *410*, 277.
- (25) Møllendal, H.; Cole, G. C.; Guillemin, J.-C. *J. Phys. Chem. A* **2006**, *110*, 921.
- (26) Wodarczyk, F. J.; Wilson, E. B., Jr. *J. Mol. Spectrosc.* **1971**, *37*, 445.
- (27) Frisch, M. J.; Trucks, G. W.; Schlegel, H. B.; Scuseria, G. E.; Robb, M. A.; Cheeseman, J. R.; Montgomery, J. A., Jr.; Vreven, T.; Kudin, K. N.; Burant, J. C.; Millam, J. M.; Iyengar, S. S.; Tomasi, J.; Barone, V.; Mennucci, B.; Cossi, M.; Scalmani, G.; Rega, N.; Petersson, G. A.; Nakatsuji, H.; Hada, M.; Ehara, M.; Toyota, K.; Fukuda, R.; Hasegawa, J.; Ishida, M.; Nakajima, T.; Honda, Y.; Kitao, O.; Nakai, H.; Klene, M.; Li, X.; Knox, J. E.; Hratchian, H. P.; Cross, J. B.; Bakken, V.; Adamo, C.; Jaramillo, J.; Gomperts, R.; Stratmann, R. E.; Yazyev, O.; Austin, A. J.; Cammi, R.; Pomelli, C.; Ochterski, J. W.; Ayala, P. Y.; Morokuma, K.; Voth, G. A.; Salvador, P.; Dannenberg, J. J.; Zakrzewski, V. G.; Dapprich, S.; Daniels, A. D.; Strain, M. C.; Farkas, O.; Malick, D. K.; Rabuck, A. D.; Raghavachari, K.; Foresman, J. B.; Ortiz, J. V.; Cui, Q.; Baboul, A. G.; Clifford, S.; Cioslowski, J.; Stefanov, B. B.; Liu, G.; Liashenko, A.; Piskorz, P.; Komaromi, I.; Martin, R. L.; Fox, D. J.; Keith, T.; Al-Laham, M. A.; Peng, C. Y.; Nanayakkara, A.; Challacombe, M.; Gill, P. M. W.; Johnson, B.; Chen, W.; Wong, M. W.; Gonzalez, C.; Pople, J. A. *Gaussian 03, revision B.03*; Gaussian, Inc.: Pittsburgh, PA, 2003.
- (28) Møller, C.; Plesset, M. S. *Phys. Rev.* **1934**, *46*, 618.
- (29) Dunning, T. H., Jr. *J. Chem. Phys.* **1989**, *90*, 1007.
- (30) Peterson, K. A.; Dunning, T. H., Jr. *J. Chem. Phys.* **2002**, *117*, 10548.
- (31) Becke, A. D. *J. Chem. Phys.* **1993**, *98*, 5648.
- (32) Lee, C.; Yang, W.; Parr, R. G. *Phys. Rev. B* **1988**, *37*, 785.
- (33) Watson, J. K. G. *Vibrational Spectra and Structure*; Elsevier: Amsterdam, 1977; Vol. 6.
- (34) Gordy, W.; Cook, R. L. *Techniques of Chemistry, Vol. XVII: Microwave Molecular Spectra*; John Wiley & Sons: New York, 1984; Vol. XVII.
- (35) Thomas, C. H. *J. Chem. Phys.* **1973**, *59*, 70.
- (36) Nakagawa, J.; Okutani, H.; Hayashi, M. *J. Mol. Spectrosc.* **1982**, *94*, 410.
- (37) Ray, B. S. *Z. Phys.* **1932**, *78*, 74.
- (38) Sørensen, G. O. *J. Mol. Spectrosc.* **1967**, *22*, 325.
- (39) Nakagawa, J.; Kuwada, K.; Hayashi, M. *Bull. Chem. Soc. Jpn.* **1976**, *49*, 3420.
- (40) Helgaker, T.; Gauss, J.; Jørgensen, P.; Olsen, J. *J. Chem. Phys.* **1997**, *106*, 6430.
- (41) Kraitichman, J. *Am. J. Phys.* **1953**, *21*, 17.
- (42) Pauling, L. *The Nature of the Chemical Bond*; Cornell University Press: Ithaca, NY, 1960.

JP101245F